Predictions of road traffic noise on residential balconies using a specular & diffusion model

Daniel Naish (1), Andy C. C. Tan (1) & Nur Demirbilek (1)

(1) Queensland University of Technology, George Street, Brisbane, Queensland, 4001. Australia.

ABSTRACT

A combined specular reflection and diffusion model using the radiosity technique was developed to calculate road traffic noise level on residential balconies. The model is capable of numerous geometrical configurations for a single balcony situated in the centre of a street canyon. The geometry of the balcony and the street can be altered for width, length and height. The surface absorption properties of the balcony and street surfaces can be configured for numerous scenarios. The model was used to calculate for three different geometrical and acoustic absorption characteristics for a balcony. The calculated results are presented in this paper.

1. INTRODUCTION

This paper presents some preliminary results of road traffic noise prediction on residential balconies using a purpose made computer program that calculates the direct path, specular reflection paths and diffuse paths of sound energy. This paper is the third in a study of road traffic noise on residential balconies. The first paper summarised key literature into this topic [1]. The second paper presented a theoretical model developed to conduct predictions of a road traffic noise on residential balconies along and standard urban street [2]. This paper extends on these two papers by presenting the results from a some more detailed investigations using a computer model developed for this purpose. For completeness, this paper briefly presents a summary of the background literature and the basis of the theoretical model and computer model.

Previous research into environmental noise on residential balconies has mainly focused on road traffic noise and has also involved a range of methods from full scale measurements in [3-7] to scale modelling in [8-14] and theoretical models in [6-9, 11-13, 15, 16]. Several benefits of acoustic treatments on balconies have been highlighted broadly in the literature. Benefits such as; (1) a spatial reduction within the balcony space and, (2) a reduction of internal noise level in an adjacent room are noted. The authors are not aware of any study which investigates the contributions of direct, specular reflection and diffuse sound energy paths for the balcony space.

2. THEORETICAL MODEL

2.1 Geometry

A series of simple planes make up the model which simulates a urban street. Most of the planes are associated with the balcony which is located near the centre of a long building façade, as indicated in Figure 1. Every plane in the model

has adjustable absorption coefficients, α, and diffusion coefficients, ζ, where it is assumed that each plane has constant properties across the entire area. A few of the balcony planes form barriers, which are used to calculate the attenuation provided by edge diffraction. The planes which comprise the balcony are shown in more detail in Figure 2.
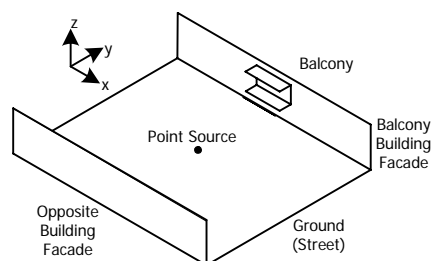

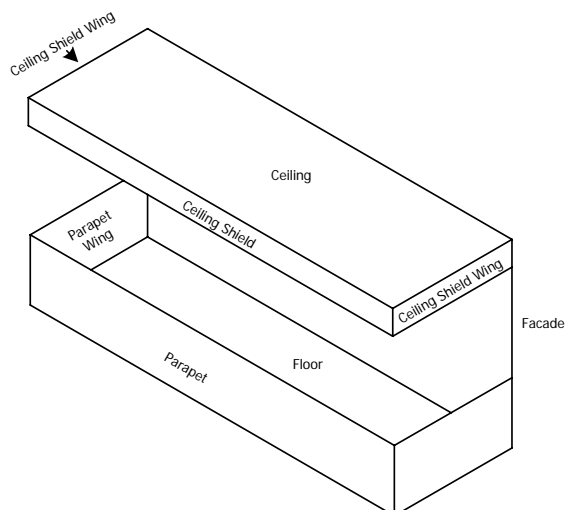**Figure 1**: Conceptual view of the model and its planes

Figure 2: Conceptual view of the balcony and its planes

2.2 Theory

Some parts of this section have been replicated in part from the previous paper [2], but condensed wherever possible.

This theoretical model includes a direct path, a specular reflection path; and a diffuse path. Geometric spreading, air absorption and barrier attenuation are included in the direct path. The specular reflection path is capable of calculating up to 10 orders of source images, and like the direct path it includes losses for geometric spreading, air absorption and barrier attenuation. The radiosity technique is implemented to calculate diffusion. Two radiosity compartments are created as indicated in Figure 3. The first radiosity compartment is the urban street, represented as a street with building facades on either side. The second radiosity compartment is the balcony space.
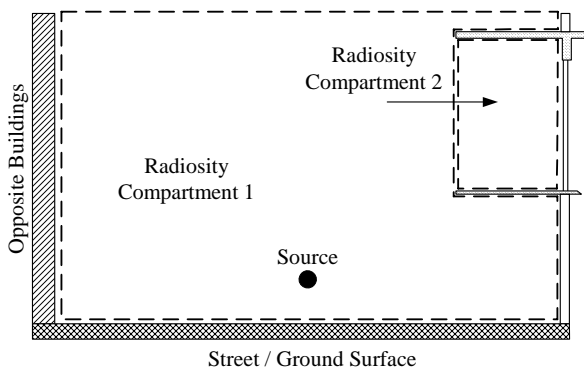

Figure 3: Two radiosity compartments for diffusion calculations.

The model is incoherent and designed to calculate sound pressure levels in 1/3 octave bands however only overall dB(A) results are presented in this paper. The arrival time of each source pulse is used to calculate the time-varying sound pressure level received so that generalised acoustic parameters and statistics may be determined.

The direct path intensity, I_d, is calculated using Equation 1 which includes losses for air absorption, ψ, and any possible barrier attenuation, δ. In Equation (1), ε is an individual point source and d_T is the total distance from source to receiver.

$$I_d = \frac{W_\varepsilon}{4\pi d_T^2} e^{-\psi d_T} - \delta \tag{1}$$

Barrier attenuation is calculated with Equation 2 using the methodology in ISO9613-2:1996 [17]. Only single diffraction is considered (that is, $C_3 = 1$) and K_{met} is ignored due to close proximity of the barriers to the receiver. As specular reflections are considered from the ground plane in the specular reflection module, the constant C_2 is equal to 40. The path difference, z, is calculated for each potential barrier plane with the highest possible path difference used to calculate δ_{dB}, which is the logarithmic form of δ. The model does not consider multiple barrier effects.

$$\delta_{dB} = 10\log_{10}\left[3 + \left(\frac{C_2}{\lambda}\right)C_3 z K_{met}\right] \text{ dB re 2e-5 Pa} \tag{2}$$

Equation 3 is used to calculate air absorption using the methodology in ISO9613-1:1993 [18] which takes into account classical losses due to viscosity and thermal effects, molecular absorption for rotational relaxation of oxygen and nitrogen molecules, molecular absorption losses for vibrational

relaxation of O_2 molecules and molecular absorption losses for vibrational relaxation of N_2 molecules.

$$\psi = \psi_{classical} + \psi_{rotational} + \psi_{O_2 vibrational} + \psi_{N_2 vibrational} \tag{3}$$

The specular path intensity, I_s, is calculated with Equation 4 which accounts for up to 10 consecutive and different reflection planes.. The subscript, a, refers to reflection plane, a.

$$I_s = \frac{W_\varepsilon}{4\pi d_T^2} e^{-\psi d_T} \sum_{a=1}^{10} \left[(1-(\alpha_a + \varsigma_a)) - \delta\right] \tag{4}$$

The radiosity method employed is described in more detail in [19, 20]. In summary, the radiosity technique utilises radiation heat transfer techniques by considering an exchange of diffuse energy from radiating planes. To account for the amount of diffuse energy radiating from a source plane to a receiver plane, the form factor, FF, is calculated. This model uses the Nusselt method described in [19], which is the ratio of the area projected from the receiver plane onto the base of a unit hemisphere located on the centroid of the source plane. Each plane is divided into a number of smaller patches, where each small patch provides diffuse energy to the receiver. Two radiosity compartments are used as indicated in Figure 3, but the method of calculation for each compartment is the same.

There are two orders of radiosity considered in this work. The first order calculates the diffuse energy intensity, I_1, at a receiver point due to a single diffuse reflection from a patch. The sound power of a plane patch, W_p, is calculated due to a direct path from the road source, ε, to patch, p, using the surface area of the patch, A_p using Equation 5. In Equation 5, d_{sp} is the distance from the road source to the centroid of the patch. Equation 6 then calculates I_1 by assuming the patch area is sufficiently small and far enough from the receiver to simulate a point source. In Equation 6, d_{pr} is the distance from the centroid of the patch to the receiver.

$$W_p = \left\{\frac{W_\varepsilon \varsigma_p}{4\pi d_{sp}^2} e^{-\psi d_{sp}} - \delta_{sp}\right\} A_p \tag{5}$$

$$I_1 = \frac{W_p}{4\pi d_{pr}^2} e^{-\psi d_{pr}} - \delta_{pr} \tag{6}$$

The second order of radiosity calculates the diffuse energy intensity, I_2, at a receiver due to a double diffuse reflection that is, from a road source to patch, i, then to another patch, j, and then to a receiver, r. Equation 7 indicates the process where W_{pa} is calculated using an identical version of Equation 5. In Equation 7, 'jr' denotes the path from patch, j, to receiver, r, and subscript 'ij' denotes the path from patch, i, to patch, j, and vice versa.

$$I_2 = \frac{\left(W_{pi} FF_{ji} \varsigma_b e^{-\psi d_{ij}} - \delta_{ij}\right)}{4\pi d_{jr}^2} e^{-\psi d_{jr}} - \delta_{jr} \tag{7}$$

3.0 COMPUTER MODELLING

A computer model was created from the geometry and theory presented in Section 2. As mentioned above a direct path, a specular reflection path; and a diffuse path is included. The programming was specifically designed such that the pulses from each type of path can be post analysed individually. This variable is defined as the Pulse Type (PT). There are 6 pulse types calculated in the model and their relative paths are shown in Figure 4. Pulse types PT1 and PT2 relate to the direct paths and specular reflection paths respectively. PT3 and PT4 are respectively the 1st order and 2nd order diffuse

paths from the radiosity compartment 1 (the street). Similarly the 1st order and 2nd order diffuse paths from radiosity compartment 2 are defined as PT5 and PT6 respectively.

In this current study, only a single point source was used in the calculations. This source was located 20m from the balcony facade. As only one point source is used, only one pulse of direct sound is possible. Depending on the geometry, the model allows up to 39 possible specular reflection paths. The ground, façade (Balcony and Balcony Building), floor, ceiling and opposite building planes allow specular reflection. Diffuse reflections are allowed from all planes within each respective compartment. A large number of pulses are calculated from the diffusion algorithms as these are not as restrictive geometrically as the requirements for a successful specular reflection. Each pulse emitted that reaches the receiver is recorded in a database with its level and the arrival time.
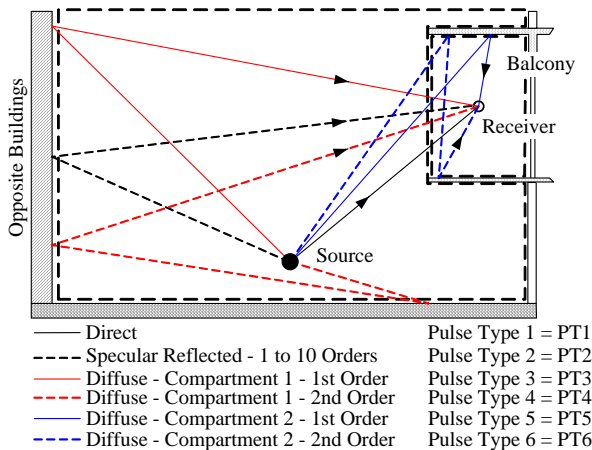
—— Direct	Pulse Type 1 = PT1
- - - Specular Reflected - 1 to 10 Orders	Pulse Type 2 = PT2
—— Diffuse - Compartment 1 - 1st Order	Pulse Type 3 = PT3
- - - Diffuse - Compartment 1 - 2nd Order	Pulse Type 4 = PT4
—— Diffuse - Compartment 2 - 1st Order	Pulse Type 5 = PT5
- - - Diffuse - Compartment 2 - 2nd Order	Pulse Type 6 = PT6

Figure 4: Some of the 39 predefined specular reflection paths.

A grid of receiver points was created across the middle of the balcony. The grid was 11x11 points (121 points total) and its arrangement is indicated in Figure 5. The coordinates were generally a uniform distance apart except near the planes of the balcony. Some of the results in the following sections are presented according to their receiver code, e.g. $z0$, $z1$, $z2...z10$ etc.
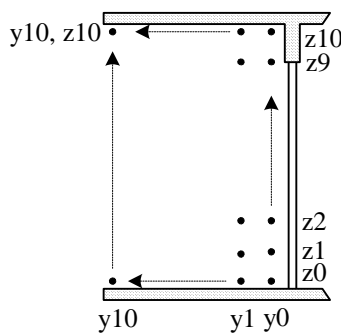
Figure 5: Receiver grid along the centre cross section of the balcony.

In this current study, the geometry of the street and the position of the balcony was fixed, only the balcony configuration was changed. The urban street modelled is represented in Figure 6. The street is 40m wide with 5m high buildings on either side. A single balcony is located on one of the buildings at a height of 2m above the flat ground plane. The

height of the balcony is 3m and its depth is 2m which is a typical usable balcony for a residential purpose. A single point source is located in the geometric centre of the ground plane, at a height of 0.5m above its surface. This is a source height typically found in traditional road traffic noise calculation methods such as CoRTN [21]. Although more modern methods have divided the propulsion and rolling noises [22] and this computer model is capable of using multiple point sources, only a single point source is needed for the purposes of this study. This study has used sound power level data obtained from a separate study by the main author. The sound power level adopted for this study was the average sound power level in 1/3 octave bands of passenger cars travelling on a dense graded asphalt pavement at 60km/hr.
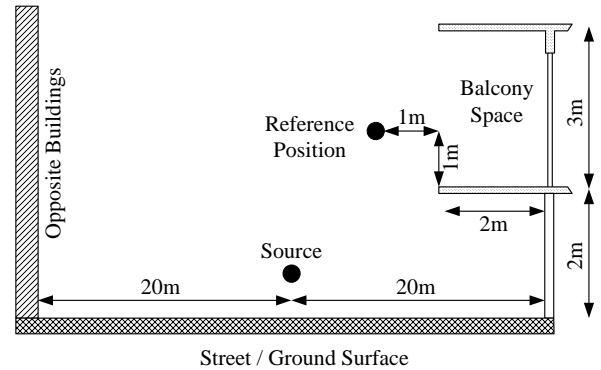
Figure 6: Geometrical arrangement for this study

This study uses a reference position which is proposed to be adopted for future prediction and measurement analysis of noise on residential balconies. The reference position is 1m above the balcony floor surface and 1m away from the protruding edge of the balcony floor, as shown in Figure 6. The position is at the midpoint of the balcony width. As most balconies are rectangular or a combination of rectangles, this location should be easy to locate on most balconies. There should be limited difficulties in finding the appropriate reference location on curved balconies.

3.1 Balcony Cases Investigated

This study investigates three different balcony designs at the same height above the ground plane and distance from the source. The cases are shown in Figure 7. Case A represents a standard balcony which does not include any acoustic treatment and is therefore considered the reference case in this study. Case B is the same as Case A except it has a 1m high parapet and an absorptive lining on the ceiling. Case C is similar to case B except it also includes 0.5m deep ceiling shield which are absorptive, an angled ceiling and an angled parapet.
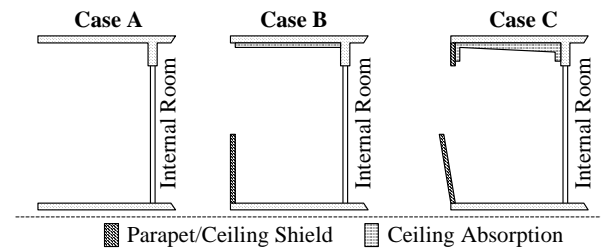
Figure 7: Balcony cases investigated in this study.

As this study is aimed at producing preliminary results for comparison between the assessed balcony cases, an extensive array of different absorption and diffusion characteristics were not included. The broadband coefficients used are shown in Table 1. The most acoustic characteristic variabil-

ity is the absorption of the balcony ceiling and ceiling shields (Case C). Diffusion coefficients have been kept constant across all cases in this current study. The model operates in 1/3 octaves, however for these preliminary results, absorption and diffusion coefficients are constant across all frequencies. Future studies will investigate the use of variably frequency coefficients.

Table 1: Absorption and Diffusion coefficients used in the study for balcony Cases, A, B and C.

	Absorption			Diffusion		
Case	A	B	C	A	B	C
Ground	5%	5%	5%	5%	5%	5%
Façade	5%	5%	5%	15%	15%	15%
Balc. Floor	5%	5%	5%	5%	5%	5%
Balc. Ceiling	5%	50%	50%	5%	5%	5%
Balc. Ballustrades	5%	5%	5%	5%	5%	5%
Ceiling Shields	5%	5%	50%	5%	5%	5%
Opposite Buildings	5%	5%	5%	15%	15%	15%

4. RESULTS

For each balcony case, calculations were performed for each receiver in the receiver grid (121 points each case). The total energy and the energy received at each receiver from each pulse type was calculated. Table 2 presents the average number of pulses calculated for each case per pulse type. Case C experiences significantly more pulses due to the increased balcony surface area from the introduction of ceiling shields. The balcony parapet exists in both Case A (0.1m high to act as diffracting edge of the balcony floor) and 1m high for Case B. This is why there is no significant differences in the pulse number between Case A and Case B.

Table 2: Number of pulses per pulse type

Case	A	B	C
PT1	1	1	1
PT2	13	13	14
PT3	150	150	150
PT4	763	765	761
PT5	100	100	225
PT6	470	471	2811
Total	1498	1500	3961

4.1 Total sound pressure levels

First of all looking at the average sound pressure level for each case and each pulse type, the average results from the receiver points adjacent to the balcony facade wall are shown in Table 3. The total average energy where $y = 0$ and $z = 0$ to 10 is 71.9dB(A) for Case A, and Case B was -3.7 dB(A) less (on average) and Case C was -4.5 dB(A) (on average). The direct path pulse type was the dominant energy source for all cases, however the dominance was less for Case B and C due to the diffraction provided by the parapet and ceiling shields. As expected, diffusion energy contributions are not appreciably different as diffusion coefficients have not changed, only the surface area of planes in the balcony compartment are increased for Case B and C.

Table 3: Average of energy near facade per pulse type, z0 to z10 dB(A)

y 0	A	B (A-B)		C (A-C)	
Total	71.9	68.2	(-3.7)	67.4	(-4.5)
PT1	70.1	65.6	(-4.6)	64.9	(-5.2)
PT2	65.8	60.7	(-5.2)	59.8	(-6.0)
PT3	56.9	54.0	(-2.9)	52.2	(-4.7)
PT4	40.5	34.3	(-6.2)	31.6	(-8.9)
PT5	55.4	55.4	(0.0)	55.1	(-0.3)
PT6	42.4	43.3	(0.9)	46.5	(4.1)

The noise level variability on the balcony facade is demonstrated in Table 4 and is compared with the noise level variability with increasing height above the balcony floor at the front of the balcony (Table 5).

Table 4: Balcony facade noise levels, z0 to z10 dB(A)

Up the rear wall, y 0	A	B	C
Z0	68.1	63.2	63.2
Z1	69.4	60.0	60.2
Z2	72.4	61.1	61.2
Z3	72.4	64.0	63.9
Z4	72.4	67.4	67.2
Z5	72.4	71.3	70.4
Z6	72.3	72.3	72.2
Z7	72.3	72.3	72.2
Z8	72.3	72.2	72.3
Z9	73.5	72.9	71.3
Z10	73.7	73.1	67.7
Average	71.9	68.2	67.4
Average Difference to Case A	0.0	-3.7	-4.5
Maximum Difference to Case A	0.0	-11.3	-11.2

Table 5: Balcony front noise levels, z0 to z10 dB(A)

Up the balcony front, y 10	A	B	C
Z0	72.9	56.5	57.5
Z1	73.4	55.9	56.9
Z2	73.3	57.0	58.4
Z3	73.3	62.2	64.2
Z4	73.2	73.2	73.1
Z5	73.2	73.2	73.1
Z6	73.1	73.2	73.1
Z7	73.1	73.1	73.1
Z8	73.1	73.1	73.0
Z9	73.0	73.0	61.5
Z10	73.0	73.0	59.3
Average	73.1	67.6	65.7
Average Difference to Case A	0.0	-5.6	-7.4
Maximum Difference to Case A	0.0	-17.5	-16.5

Firstly looking at Table 4 Case B and C both have significantly lower noise levels just above the floor which is due to the parapet diffracting edge. This difference is maintained until around z5 and z6 where the effects of the diffracting edge diminishes. Above z6 the noise level is the same for Case A and B, however the effect of the ceiling shields is observed at position z10 for Case C.

Inspecting the results in Table 5, it is observed that there are very significant reductions provided by the parapet up to position z4 for Cases B and C with more than 15 dB(A) attenuation being provided. The ceiling shields in Case C are effective at positions z9 and z10, providing over 10 dB(A) reduction in this area of the balcony space.

It is often easier to present noise levels over a surface through the use of contour maps. Noise level contours were prepared for each case and each pulse type of the total overall energy and total energy within each pulse type. These contours are shown in Figure 8 and pictorially demonstrate the attenuation effects predicted from the parapet and ceiling shield configurations in Case B and C. In Figure 8 the lines of diffraction in the contours in (a) are blurry compared to the sharpness observed in (b) and (c). This demonstrates the increasing dominance of the diffusion energy arriving from the two separate radiosity compartments where the direct and specular reflected sound has been significantly attenuated by the shadow zone of the diffracting edges. This effect is most noticeable in the corner of the parapet and balcony floor. The specular reflected energy shown in Figure 8 (c) is more attenuated than observed in Figure 8 (b) due to absorption and diffusion losses occurring prior to arrival at the receiver. The effect of ceiling reflection is observed most clearly in Case A (c) with a higher noise level in a region near the corner of the

balcony facade and ceiling. The effect of the diffracting edges is clear in Case B (c) and Case C (c), however due to the increased number of pulse arrivals the levels of attenuation are less.
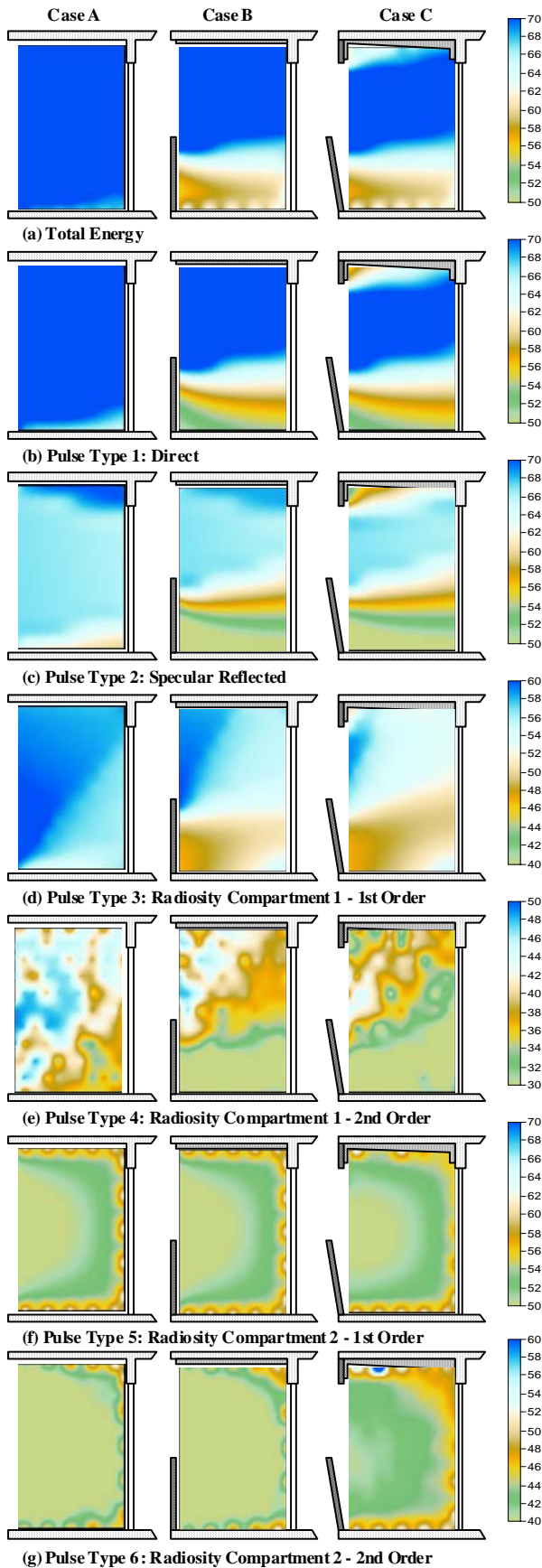

Case A   **Case B**   **Case C**

(a) Total Energy

(b) Pulse Type 1: Direct

(c) Pulse Type 2: Specular Reflected

(d) Pulse Type 3: Radiosity Compartment 1 - 1st Order

(e) Pulse Type 4: Radiosity Compartment 1 - 2nd Order

(f) Pulse Type 5: Radiosity Compartment 2 - 1st Order

(g) Pulse Type 6: Radiosity Compartment 2 - 2nd Order

Figure 8: Predicted noise level contours (dB(A)) over a cross section of the balcony for each case per pulse type.

Figure 8 (d) shows the energy distribution from the 1st order pulses from radiosity compartment 1 and again the effect of the diffracting edges is clear. Interesting to note is the relatively random directions of arriving pulses from the urban street provide a different diffraction attenuation pattern compared to the direct and specular reflected pulses. The shadowing effect of the floor and parapet edges is more vertical, indicating the significance of the 1st order diffuse energy arriving from the street surface. The 2nd order diffuse energy pulse from radiosity compartment 1 are shown in Figure 8 (e) which as expected shows a increasingly random nature of direction of arrival of sound pulses. Despite this increasing randomness, the effects of diffracting edges is also observed to attenuate 2nd order diffuse energy arriving from the surfaces near the street and lower portions of the building facades.

The contours of energy from pulses in radiosity compartment 2 (the balcony space) are shown in Figure 8 (f) and (g) for the 1st and 2nd order respectively. These contours show increased diffuse energy near the internal surfaces of the balcony space. No significant differences are observed in predicted noise levels between the balcony configuration cases from compartment 2, which is expected as no differences in diffusion were entered into the model.

4.2 Comparisons with the reference Location

Predictions were made to the reference location identified in Figure 6. The predicted total sound pressure levels at this location were 74.2 dB(A), 74.1 dB(A) and 74.1 dB(A) for Cases A, B and C respectively. Thus, the sound pressure level at the reference location is reasonably independent of the balcony geometrical and acoustical configuration. The predicted levels at each position in the balcony space receiver grid were subtracted from the level at the reference position for their respective balcony configuration case. The tabulated results are presented in Table 6 for the receiver positions at the centre of the balcony (y=5) and for each calculated height above the balcony floor (z0 to z10).

Table 6 shows the difference between the total energy at the reference location and the total energy for each point and also for each pulse type at the centre of the balcony. Figure 9 shows the same information as contours over the entire cross-section of the balcony space. For each case, the average difference for all heights above the balcony floor is calculated. In this table it is observed that where there is little or no attenuation from diffracting edges then the overall levels at centre of balcony is around 1.5 dB(A) less than the reference location and the direct energy is typically 2.8dB(A) less than the reference location. The range of attenuation to the direct path (PT1) provided by the parapet is approximately 0dB(A) to 20dB(A) and the ceiling shields provide approximately 0dB(A) to 10dB(A) attenuation.

The overall levels from the specular reflection path (PT2) are within 10dB(A) for receivers which are not afforded any significant diffracting edge attenuation. Therefore the specular reflection energy will add a noticeable increase to the overall level when expressed in decibels. The same cannot be stated for the diffuse pulse types, where there overall levels are all more than 10dB(A) lower than the reference position. Thus the relative importance of the diffusion component of the sound energy arriving at the receiver is not its impact on the overall level, but rather in the timing of its arrival and its contribution to the reverberation time of the balcony space as the diffuse levels tend to range between 15dB(A) to 35dB(A) lower than the reference position. Reverberation time of the balcony spaces will be investigated in a future study by the authors.

Table 6: Noise level difference with the reference location, dB(A) (Balcony level minus reference position) (PT = Pulse Type)

	Total	PT1	PT2	PT3	PT4	PTt5	PT6
Case A							
Z0	-5.4	-7.6	-13.0	-20.1	-37.9	-12.7	-27.3
Z1	-1.7	-2.9	-8.6	-18.1	-35.3	-20.9	-33.9
Z2	-1.4	-2.8	-7.6	-17.0	-32.8	-22.5	-36.0
Z3	-1.4	-2.8	-7.6	-16.4	-30.8	-23.4	-37.1
Z4	-1.4	-2.8	-7.6	-15.8	-28.6	-23.8	-38.0
Z5	-1.4	-2.8	-7.7	-14.8	-27.0	-24.0	-36.8
Z6	-1.4	-2.8	-7.7	-15.0	-27.2	-23.9	-37.3
Z7	-1.4	-2.9	-7.7	-15.3	-27.4	-23.5	-36.2
Z8	-1.5	-2.9	-7.7	-15.5	-34.9	-22.7	-34.6
Z9	-1.3	-2.9	-7.0	-15.7	-28.2	-21.1	-33.7
Z10	-0.1	-3.0	-4.0	-16.1	-39.6	-13.0	-24.9
Average	-1.7	-3.3	-7.8	-16.4	-31.8	-21.0	-34.2
Case B							
Z0	-11.5	-21.0	-26.2	-24.1	-50.1	-12.8	-25.0
Z1	-15.6	-19.2	-24.4	-24.6	-49.8	-20.9	-33.9
Z2	-13.9	-16.1	-21.4	-24.8	-47.1	-22.5	-35.8
Z3	-9.7	-11.2	-16.7	-23.6	-41.0	-23.4	-36.3
Z4	-5.7	-7.1	-11.9	-20.7	-38.3	-23.9	-37.7
Z5	-1.5	-2.8	-7.7	-18.3	-37.6	-24.0	-37.3
Z6	-1.5	-2.8	-7.7	-18.0	-35.7	-23.9	-37.1
Z7	-1.5	-2.9	-7.7	-17.6	-32.2	-23.5	-37.3
Z8	-1.5	-2.9	-7.8	-17.4	-31.8	-22.7	-35.7
Z9	-1.4	-2.9	-7.4	-17.3	-32.2	-21.1	-33.9
Z10	-0.7	-3.0	-5.6	-16.7	-29.5	-13.0	-27.5
Average	-5.9	-8.4	-13.1	-20.3	-38.7	-21.1	-34.3
Case C							
Z0	-11.3	-20.6	-25.9	-24.2	-44.2	-12.7	-21.9
Z1	-15.3	-18.8	-24.1	-24.8	-49.5	-20.9	-29.7
Z2	-13.6	-15.8	-21.2	-25.4	-43.9	-22.4	-31.6
Z3	-9.9	-11.3	-16.9	-25.2	-43.9	-23.2	-32.0
Z4	-6.0	-7.5	-12.1	-23.6	-40.2	-23.6	-31.6
Z5	-1.6	-2.9	-7.8	-21.2	-37.0	-23.7	-32.0
Z6	-1.5	-2.8	-7.7	-20.1	-37.5	-23.6	-31.6
Z7	-1.6	-2.9	-7.7	-19.9	-34.6	-23.1	-30.8
Z8	-1.6	-2.9	-7.8	-19.5	-33.5	-22.1	-30.3
Z9	-5.8	-7.6	-11.5	-20.0	-43.7	-20.1	-28.5
Z10	-6.6	-10.8	-14.9	-21.4	-45.0	-10.7	-19.8
Average	-6.8	-9.5	-14.3	-22.3	-41.2	-20.6	-29.1

The contours in Figure 9 show the difference between the reference position level and the level calculated across the balcony space receiver grid. The scale in the contours shows a thin black line where there is 0 dB(A) difference with the reference position level. The total energy contours in Figure 9 (a) clearly shows the zones in the balcony space where attenuation is provided by the parapets and ceiling shields. The attenuation effect of these diffracting edges is observable also in the diffuse energy arriving from radiosity compartment 1 (the street). The diffuse energy from the 2nd order radiosity paths (Figure 9 (e) and (g)) is mostly more than 30 dB(A) lower than the reference position. The 1st order diffuse energy from radiosity compartment 2 (the balcony) demonstrates in Figure 9 (f) the relatively higher levels nearer to the internal surfaces of the balcony space. The variability in the diffuse energy observed in Figure 9 (d) and (f) is an indication that there will be differences in an impulse decay curve across the balcony space contributed by diffuse energy from both radiosity compartments 1 and 2.

It is worthwhile noting that the reference position receiver was always higher in level than any of the balcony space receivers. It is essential in this study and future studies to consider the reference position, as the reference position will be an essential variable in any possible compliance testing

framework developed for the measurement of road traffic noise levels on balcony spaces.
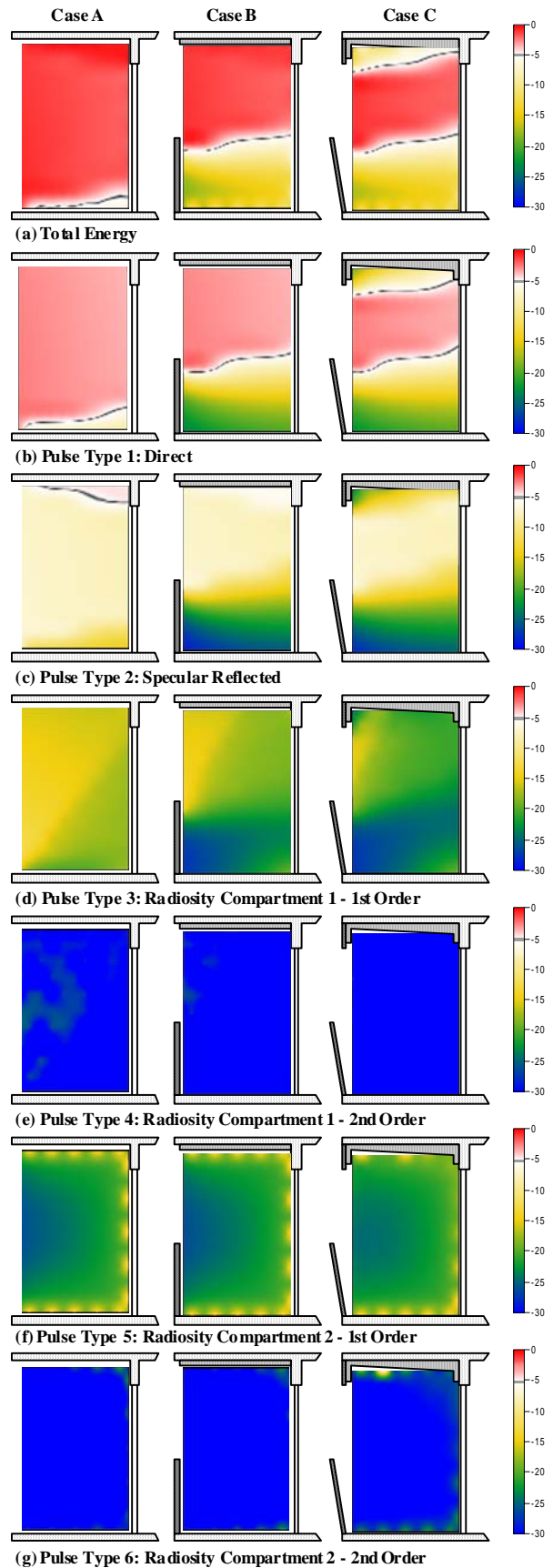

(a) Total Energy

(b) Pulse Type 1: Direct

(c) Pulse Type 2: Specular Reflected

(d) Pulse Type 3: Radiosity Compartment 1 - 1st Order

(e) Pulse Type 4: Radiosity Compartment 1 - 2nd Order

(f) Pulse Type 5: Radiosity Compartment 2 - 1st Order

(g) Pulse Type 6: Radiosity Compartment 2 - 2nd Order

Figure 9: Contours of the difference in levels between then reference position and the balcony space, dB(A).

5. CONCLUSIONS

This study has continued research into the area of road traffic noise on balcony spaces. In using a specifically designed computer model which includes direct sound paths, specular reflection paths and four diffuse sound paths, it has been possible to explore the acoustic characteristics of different balcony configurations.

The results of this study have shown the levels of attenuation that can be expected from solid balcony parapets and ceiling shields and with strategic placement of absorptive surfaces.

This study has not attempted to cover a more diverse range of balcony geometries or acoustic configurations (absorption and diffusion) as the current purpose has been to demonstrate the outputs of the developed theoretical and computer model. These results show the dominance of the paths of sound energy and their contribution to the total energy at a particular receiver within the balcony space.

Future work is intended in using the developed computer model to investigate a wide range of balcony and urban street geometries and acoustic characteristics. Further investigation will be made into the locations of the road traffic noise source i.e. near the balcony and far away down the street. The effects of these changes on the reverberation time within the balcony space will also form part of the future investigations.

REFERENCES

1.   Naish, D. and A.C.C. Tan, 2007. *A review of residential balconies with road traffic noise.* in *14th International Congress on Sound and Vibration.* Cairns, Australia,

2.   Naish, D. and A.C.C. Tan, 2008. *Residential balconies with road traffic noise: A combined source image and radiosity model.* in *15th International Congress on Sound and Vibration.* Daejeon, Korea,

3.   Gustafsson, J.-I. and S. Einarsson, 1973. *Gallery houses with respect to traffic noise.* in *Inter-noise 73.* Copenhagen, The British Library.

4.   May, D.N., 1979. *Freeway noise and high-rise balconies.* Journal of the Acoustical Society of America, 65 (3): p. 699-704.

5.   Tzekakis, E.G., 1983. *On the noise reducing properties of balconies.* Acustica, 52 (2): p. 117-21.

6.   Li, K.M., et al., 2003. *A simple formula for evaluating the acoustic effect of balconies in protecting dwellings against road traffic noise.* Applied Acoustics, 64 (7): p. 633-653.

7.   Lee, P.J., et al., 2007. *Effects of apartment building facade and balcony design on the reduction of exterior noise.* Building and Environment, 42 (10): p. 3517-3528.

8.   Mohsen, E.A. and D.J. Oldham, 1977. *Traffic noise reduction due to the screening effect of balconies on a building facade.* Applied Acoustics, 10 (4): p. 243-257.

9.   Oldham, D.J. and E.A. Mohsen, 1979. *A model investigation of the acoustical performance of courtyard houses with respect to noise from road traffic.* Applied Acoustics, 12 (3): p. 215-30.

10.   Hammad, R.N.S. and B.M. Gibbs, 1983. *The acoustic performance of building facades in hot climates: Part 2--Closed balconies.* Applied Acoustics, 16 (6): p. 441-454.

11.   Cheng, W.F., C.F. Ng, and K.C. Fung, 2000. *The theoretical model to optimize noise barrier performance at the window of a high-rise building.* Journal of Sound and Vibration, 238 (1): p. 51-63.

12.   Kropp, W. and J. Berillon, 2000. *Theoretical model to consider the influence of absorbing surfaces inside the cavity of balconies.* Acta Acustica (Stuttgart), 86 (3): p. 485-494.

13.   Hossam El Dien, H. and P. Woloszyn, 2005. *The acoustical influence of balcony depth and parapet form: experiments and simulations.* Applied Acoustics, 66 (5): p. 533-551.

14.   Tang, S.K., 2005. *Noise screening effects of balconies on a building facade.* Journal of the Acoustical Society of America, 118 (1): p. 213-221.

15.   Hothersall, D.C., K.V. Horoshenkov, and S.E. Mercy, 1996. *Numerical modelling of the sound field near a tall building with balconies near a road.* Journal of Sound and Vibration, 198 (4): p. 507-515.

16.   Hossam El Dien, H. and P. Woloszyn, 2004. *Prediction of the sound field into high-rise building facades due to its balcony ceiling form.* Applied Acoustics, 65 (4): p. 431-440.

17.   ISO9613-2, 1996. *ISO9613-2 Acoustics - Attenuation of sound during propagation outdoors - Part 2: General method of calculation.*

18.   ISO9613-1, 1993. *ISO9613-1 Acoustics - Attenuation of sound during propagation outdoors - Part 1: Calculation of the absorption of sound by the atmosphere.*

19.   Kang, 2007. *Urban Sound Environment.* ed. Vol. New York: New York.

20.   Lewers, T., 1993. *A Combined Beam Tracing and Radiant Exchange Computer-Model of Room Acoustics.* Applied Acoustics, 38 (2-4): p. 161-178.

21.   Department of Transport Welsh Office, 1988. *Calculation of Road Traffic Noise.* ed. Vol. London: Her Majesty's Stationery Office.

22.   Harmonoise, 2005. *Technical Report HAR32TR-040922-DGMR20 Harmonoise WP 3 Engineering method for road traffic and railway noise after validation and fine tuning.*